Electronic Supplementary Material (ESI) for Journal of Materials Chemistry A.

Supporting Information

Chemically Designed CeO_2 Nanoboxes Boost the Catalytic Activity of Pt Nanoparticles toward Electro-oxidation of Formic Acid

Swetha Ramani,[†] Sumanta Sarkar,[†] Vamseedhara Vemuri, Sebastian C Peter*

New Chemistry Unit, Jawaharlal Nehru Centre for Advanced Scientific Research, Bangalore 560064, India

*E-mail: sebastiancp@gmail.com, sebastiancp@jncasr.ac.in

† These authors contributed equally

Experimental Methods

S2.1 Chemicals

Copper chloride ($CuCl_2$, anhydrous, 99%), cerium ammonium nitrate pentahydrate ($(NH_4)_2Ce(NO_3)_6$, 99%), HNO_3, polyvinyl-2-pyrrolidone (PVP), potassium chloroplatinate (K_2PtCl_4) and chloroplatinic acid ($H_2PtCl_6.6H_2O$) were purchased from Alfa Aesar. Copper sulphate pentahydrate ($CuSO_4.5H_2O$, extrapure AR) was purchased from SRL chemicals. Tri sodium citrate dihydrate (99%) was purchased from Sigma Aldrich. All the reagents were used without further purification. Deionized water (TKA, 18.2 MΩ.cm) was used throughout the syntheses and measurements.

S2.2 Synthesis

S2.2.1 Synthesis of 200 nm Cu_2O Nanocubes (Cu_2O_NC(200 nm))

Cu_2O_NC(200 nm) with an approximate edge length of 200 nm were synthesized using the strategy outlined by Zhang *et al.*[1] A 100 mL aqueous solution of $CuCl_2$ (0.01 M) was slowly hydrolyzed with 10 mL 2.0 M aqueous NaOH solution. The solution immediately turned turbid (blue in color) and was stirred for 30 min. An aqueous solution of 10 mL 0.6 M ascorbic acid was added dropwise. The final solution was stirred at 55 °C for 5 h. The resulting precipitate in bright orange color which was collected by centrifugation (6000 rpm), washed with distilled water for 3-4 times, and finally vacuum dried at room temperature for 24 h.

S2.2.2 Synthesis of 50-150 nm Cu_2O Nanocubes (Cu_2O_NC(50-150 nm))

Various sizes of **Cu_2O_NC** with were synthesized by a similar strategy reported in the literature.[2] The reduction of $Cu(OH)_2$ was done using ascorbic acid in the presence of different amounts of sodium citrate. The synthetic conditions varied for different sizes include

$CuSO_4$:$C_6H_5Na_3O_7.2H_2O$:NaOH in the ratio 1:0.25:4, 1:1:4 and 1:1.25:4 for 50, 100 and 150 nm, respectively.

S2.1.2.3 Synthesis of CeO_2@Cu_2O Core-Shell Nanocubes (Cu_2O@CeO_2 CS-NC)

A template assisted route reported by Bao *et al*[3] was employed for the synthesis of **Cu_2O@CeO_2 CS-NC**. In a typical synthesis, 0.855 M NaCl aqueous solution was added to a suspension of the synthesized Cu_2O nanocubes in ethanol. The suspension was adequately dispersed for 30 min under ultrasonication. The $(NH_4)_2Ce(NO_3)_6$ ethanol solution (0.4 mM) was added to the above suspension dropwise at 40 °C in an oil bath under vigorous stirring. The reaction was allowed to proceed for an additional 1 hr at the same reaction condition. The solid product was collected by several rinse−centrifugation (5000 rpm) cycles and then dried in vacuum at room temperature. For different CeO_2 shell thickness, the 0.4 mM $(NH_4)_2Ce(NO_3)_6$ was varied from 0.2-1.0 mM.

S2.1.2.3 Synthesis of Pt on Cu_2O@CeO_2 Core-Shell Nanocubes (Pt/(Cu_2O@CeO_2 CS-NC)

In a typical synthetic operation, the yield obtained from the second step (synthesis of **Cu_2O@CeO_2 CS-NC**) were ultrasonically dispersed in 20 mL doubly distilled water. Appropriate amounts of K_2PtCl_4 aqueous solution was added to the suspension. The reaction was initiated by adding 3-4 drops of glacial acetic acid under constant sonication. The solution immediately turned black, indicating the formation of platinum nanoparticles. The reaction was maintained undisturbed for 1 h and the black precipitate was collected by centrifuging and rinsing with doubly distilled water to remove generated Cu^{2+} ions.

S2.1.2.4 Synthesis of Pt on CeO_2 Nanoboxes (Pt/CeO_2_NB)

In order to obtain **Pt/CeO_2_NB**s, the product obtained from the above reaction was etched with 1 M HCl for 2-3 h to completely get rid of the Cu_2O template.

S2.1.2.5 Synthesis of 50 nm Pt Nanoboxes (Pt_NB)

Pt_NBs with an average edge length of 50 nm was synthesized using the same synthetic procedure as in the case of **Pt/CeO_2_NB**s without the addition of $(NH_4)_2Ce(NO_3)_6$.

S2.1.2.6 Synthesis of Solid CeO_2 Nanocubes (CeO_2_SC)

A modified version of the synthetic strategy reported by Yang *et al*[4] was utilized in order to synthesize ~50 nm **CeO_2_SC**. An aqueous solution of 30 mL 10.6 M NaOH was rapidly added to another aqueous solution of 10 mL 0.23 M $Ce(NO_3)_3 \cdot 6H_2O$ under vigorous stirring resulting in a light yellow slurry. The mixture was further stirred for 30 min and finally transferred to a 50 mL autoclave filled 80% with doubly distilled water and the above contents were transferred into it. The autoclave was heated at 180 °C for 24 h and was then allowed to cool to room temperature normally. The grayish product was collected by centrifugation at 5000 rpm and subsequent washing with doubly distilled water and dried at 60 °C.

S2.1.2.7 Synthesis of Hollow CeO_2 Nanospheres (CeO_2_HNS)

Monodispersed hollow **CeO_2_HNS** were synthesized using a protocol previously reported by Yang *et al.*[5] In a typical synthesis of **CeO_2_HNS**, 0.1 g of $CeCl_3$, $7H_2O$ and 0.18 g of PVP were dissolved in 19 mL of deionized water under vigorous magnetic stirring. 1 mL of formamide and 0.1 mL of H_2O_2 were then added into the solution under continuous stirring for 30 min. The as-formed yellow solution was transferred into a teflon-lined autoclave of 23 mL capacity and heated for 24 h at 180 ^{o}C. After the autoclave was cooled to room temperature naturally, light brown products were collected and washed with deionized water 4 times. Finally, the products were washed with absolute ethanol and dried in an electric oven for 6 h at 70 ^{o}C.

S2.1.2.8 Synthesis of Pt on CeO_2 solid cubes and hollow nano spheres (Pt/CeO_2_SC and Pt/CeO_2_HNS)

CeO_2_SC and CeO_2_HNS (10 mg in each case) were dispersed in 10 mL deionized water under ultrasonication and then mixed with appropriate amounts of K_2PtCl_4 solution under vigorous stirring for 1 h. Finally, K_2PtCl_4 was reduced to metallic Pt with the addition of a reducing agent $NaBH_4$ (5 wt%) under stirring for another 1 h.

S2.1.2.9 Sample Preparation for electrochemistry

All the samples were supported on Vulcan XC-72R by taking appropriate amount of the catalyst such that final Pt loading was maintained as 0.01 mg and 0.5 mg of Vulcan XC-72R in 1 mL isopropanol/water (1:1 v/v) mixture and ultrasonicated for 30 min.

S2.1.2.10 Preparation of Pt/CeO_2_NB on reduced grapheme oxide (Pt/CeO_2_NB/RGO)

Reduced graphene oxide was synthesized using a modified Hummers method.[6, 7] Graphite flakes 500 mg in a 250 mL round bottom flask and then 12 mL of H_2SO_4 and 12 mL HNO_3 were slowly added to it at low temperature (0–5 °C) with constant stirring. This was followed by addition of 1.5 g of $KMnO_4$. The temperature was slowly raised to 35 °C and stirred for 30 min. Water (22 mL) was then added slowly to the thick slurry. The temperature was further raised to 98 °C and kept for another 15 min. The mixture was diluted to 66 mL with warm water after cooling it down to room temperature. Finally, 30 mL of 30% H_2O_2 was added to it. The brown colored product was filtered and washed repeatedly with 1 M HCl to get rid of the ions, followed by rigorous washing with hot distilled water. Then it was collected in a dialysis bag (12000 DA) and dialyzed for 7 days to bring the pH close to 5. The final product graphite oxide (GO) was collected and dried in a vacuum oven at 80 °C. To obtain rGO, 100 mg of GO was dispersed in 100 mL of water followed by the addition of 1 mL 85% hydrazine monohydrate. The dispersion was then refluxed for 5 h. The black precipitate was washed thoroughly with distilled water and dispersed in distilled water by ultrasonication for 1 h to obtain 1 mg/ mL reduced graphene oxide (rGO).

In order to synthesize **Pt/CeO_2_NB/RGO** with 20% Pt loading, a dispersion of 5 mg **Pt/CeO_2_NB** in 1 mL isopropanol was rapidly added to 1 mL aqueous dispersion of rGO under vigorous stirring followed by ultrasonication for 30 min.

S2.3 Powder X-ray Diffraction (PXRD)

PXRD measurements were done at room temperature on a Rigaku Miniflex X-ray diffractometer with a Cu−Kα X-ray source (λ = 1.5406 Å), equipped with a position sensitive detector in the angular range of $10° \leq 2\theta \leq 90°$ with the step size 0.02° and a scan rate of 0.5 s/step calibrated against corundum standards. The experimental patterns were compared to the pattern calculated from the single crystal structure refinement.

S2.4 Elemental Analysis

Quantitative microanalysis on all the samples was performed with an FEI NOVA NANOSEM 600 instrument equipped with an EDAX instrument. Data were acquired with an accelerating voltage of 20 kV and a 100 s accumulation time. The EDAX analysis was performed using the P/B-ZAF standardless method (where Z = atomic no. correction factor, A = absorption correction factor, F = fluorescence factor, P/B = peak to background model) on selected spots and points.

S2.5 Transmission Electron Microscopy (TEM)

TEM images and selected area electron diffraction (SAED) patterns were collected using a JEOL 200 TEM instrument. Samples for these measurements were prepared by sonicating the nanocrystalline powders in ethanol and dropping a small volume onto a carbon-coated copper grid.

S2.6 X-ray Photoelectron Spectroscopy (XPS)

XPS measurement was performed on an Omicron Nanotechnology spectrometer using a Mg−Kα (1253.6 eV) X-ray source with a relative composition detection better than 0.1%.

S2.7.1 Electrochemical Studies

A three-electrode setup was used with a glassy carbon electrode with a diameter 3 mm as working electrode, platinum wire as counter electrode, and Ag/AgCl (1 M KCl) as reference electrode. All the solutions were purged with nitrogen gas for 20 min prior to measurement. The catalyst ink was prepared by dispersing 2.5 mg of catalyst in 1 mL of mixed solvent solution (IPA:H2O = 1:1 v/v) and 10 μl of 0.05 wt % Nafion binder. The Nafion binder (Sigma

Aldrich, 5 wt %) was diluted to 0.05 wt % with isopropyl alcohol (IPA). A 20 μl aliquot of the catalyst ink was drop casted onto a glassy carbon (GC) electrode and dried overnight at room temperature. Before depositing the catalyst, the GC was polished with 0.05 μm alumina slurry and washed several times with distilled water (18.2 MΩcm), and IPA. Commercial Pt/C (20 wt%, Sigma Aldrich) was used for comparison of activity with the **Pt/CeO$_2$_NB**s catalyst. The blank cyclic voltammetry (CV) measurement was carried out in 0.1 M $HClO_4$ aqueous solution at a scan rate 50 mV/s. CV and chronoamperometry (CA) were performed in 0.1 M $HClO_4$/1 M FA electrolyte solution at a scan rate 50 mV/s. We have maintained the same loading of Pt (0.01 mg) in all the catalysts.

S2.7.2 Calculation of ECSA

Electrochemically Active Surface Area (ECSA) was calculated considering the hydrogen desorption region from the CV curves obtained to check catalyst stability. The charge obtained from hydrogen desorption peak was integrated considering the value of 210 μC/cm^2 for Pt based catalyst.[8]

Table S1. Illustrates the specific activity at a particular overpotential for various samples with its ECSA values.

Sample	ECSA (m^2/g)	Overpotential at peak (V) vs Ag/Agcl	Specific Activity (2nd cycle) (mA/cm^2)	Overpotential at peak (V) vs Ag/Agcl	Specific Activity (100th cycle) (mA/cm^2)	Overpotential at peak (V)	Specific Activity (250th cycle) (mA/cm^2)
Pt/CeO_2_NB (50 nm)	22.75	0.845	4.520	0.745	2.287	0.765	1.670
Pt/CeO_2_NB (100 nm)	15.60	0.875	1.787	0.815	1.177	0.775	0.921
Pt/CeO_2_NB (150 nm)	13.77	0.795	1.723	0.775	1.574	0.745	1.244
Pt/CeO_2_NB (200 nm)	3.40	0.725	1.608	0.735	1.126	0.705	0.689
Pt/CeO_2_HNS	1.38	0.743	0.766	0.675	0.114	-	-
Pt/CeO_2_SC	2.06	0.692	1.713	0.735	0.749	-	-
Pt_NB	18.55	0.818	1.783	0.755	0.522	-	-
Pt/C	18.50	0.746	0.905	0.735	0.663	-	-
Pt/CeO_2_NB/rGO	13.70	0.782	1.159	0.725	0.639	-	-

Note: CV measurements were performed only till 100 cycles. Therefore overpotential and specific activity are not mentioned in few cases for 250th cycle.

Table S2. The surface area and pore volume of Pt, Ce and Cu acquired in different samples from BET (error value in parenthesis), respectively.

Sample	Surface Area (m^2/g)	Pore volume(cc/g)
Pt/CeO$_2$_NB(50)	62.9	0.142
Pt/CeO$_2$_NB(100)	49.8	0.070
Pt/CeO$_2$_NB(150)	39.4	0.085
Pt/CeO$_2$_NB(200)	30.2	0.060
Pt/CeO$_2$_HNS	8.4	0.084
Pt/CeO$_2$_SC	45.4	0.1153

Table S3 : Illustrates the specific activity at peak potential for Pt/CeO$_2$_NB(50 nm) for MeOH and EtOH oxidation with its ECSA values.

Sample	Oxidation reaction	ECSA (m^2/g)	Peak Potential	Specific Activity (2nd cycle) (mA/cm^2)	Overpotential (V)	Specific Activity (250th cycle) (mA/cm^2)
Pt/CeO$_2$_NB	MO	17.20	0.725	0.756	0.665	1.105
Pt/C		4.33	0.701	0.497	0.709	0.502
Pt/CeO$_2$_NB	EO	2.40	-0.205	1.113	-0.205	5.337
Pt/C		8.80	-0.165	5.204	-0.195	3.247

Table S4: Specific activity of already reported Pt, Pd compounds for FAO, MOR and EOR.

S.No	Reaction	Catalyst	Specific activity (mA/cm^2)	Ref
1	**FAO**	Pt-Cu cubic	3.0	9
2		Pt$_{80}$Cu$_{20}$	2.15-2.29	10
3		Pt–Cu(1:1.2)/RGO	2.08	11
4		Pd$_6$Co/3DG	0.80	12
5		Pd-P/carbon cloth	4.9	13
1	**MOR**	Pt$_3$Cu(icosahedra)	2.14	14
2		Pt-Zn NCs (spherical)	0.90	15
3		Pt$_{60}$Cu$_{40}$	4.90	16
4		Pt-Cu nanocrystals	0.96	17
5		Pt-Cu nanocubes	4.70	18
6		PtPd/PPy/PtPd TNTAs	0.90	19
7		Au$_{oct}$@PdPt NPs	2.19	20
8		Pt-Pd NCs	1.49	21
9		Pd-Ni-Pt NPs	~0.80	22
1	**EOR**	PtRhSnO$_2$/C	7.50	23
2		PtPd/PPy/PtPd TNTAs	2.50	19
3		Pd-Ni-Pt NPs	~7.00	22

Figures

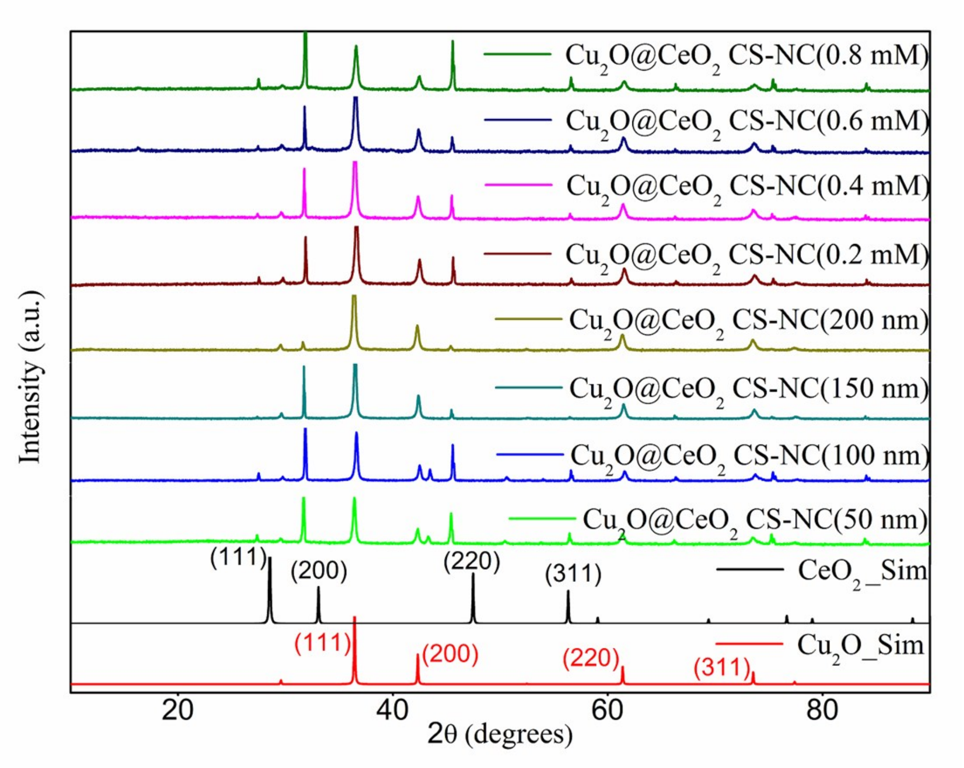

Figure S1: The comparison of powder XRD patterns of $Cu_2O@CeO_2$ CS-NCs synthesized using template assisted colloidal method for Ce concentration and nanocube size dependent study.

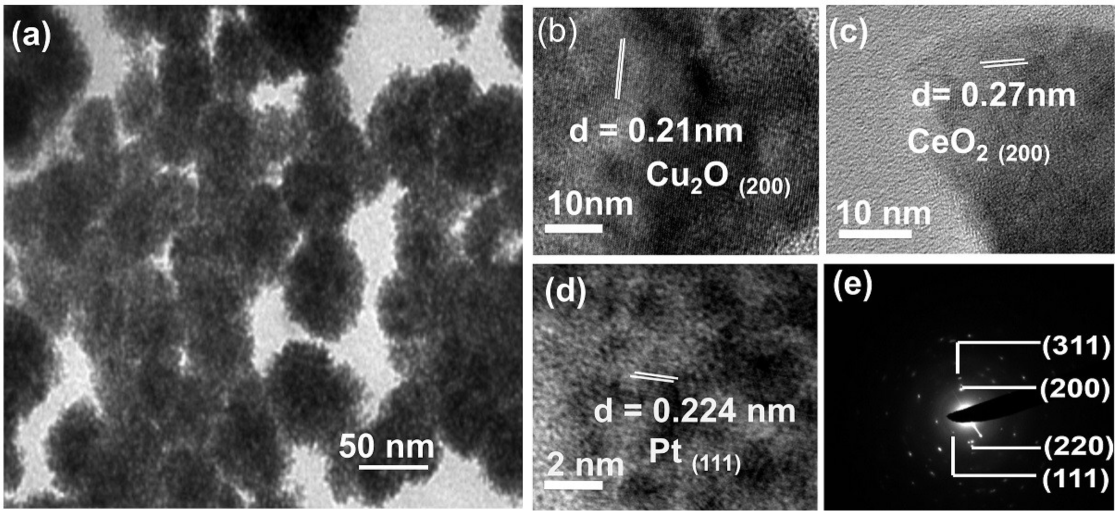

Figure S2: (a) A TEM image exhibiting the uniformity of size Pt/CeO_2_NB(50 nm), (b) HRTEM image of 50 nm Cu_2O template showing (200) plane, (c) HRTEM of CeO_2 (200) on $Cu_2O@CeO_2$ CS-NC, (d) exposed plane of Pt (111) on CeO_2_NBs and (e) SAED displays the different planes corresponding to Pt (indexed pattern on Figure S2a).

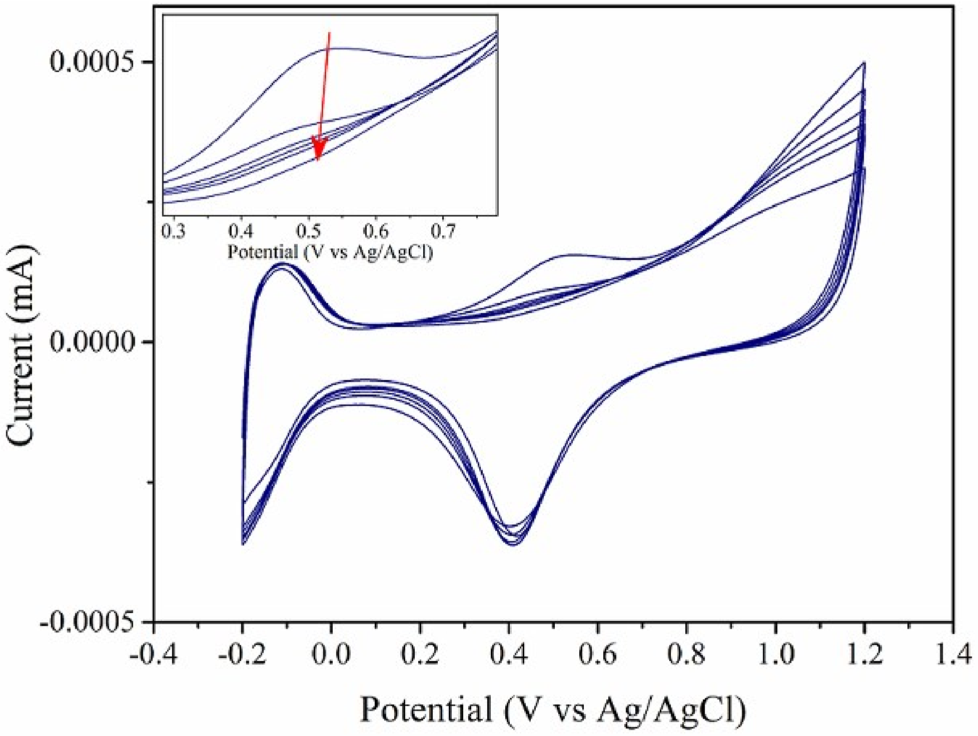

Figure S3. A characteristic CV curve of the catalyst in 0.1M $HClO_4$ showing the disappearance of Cu-O oxidation peak during repeated cycling.

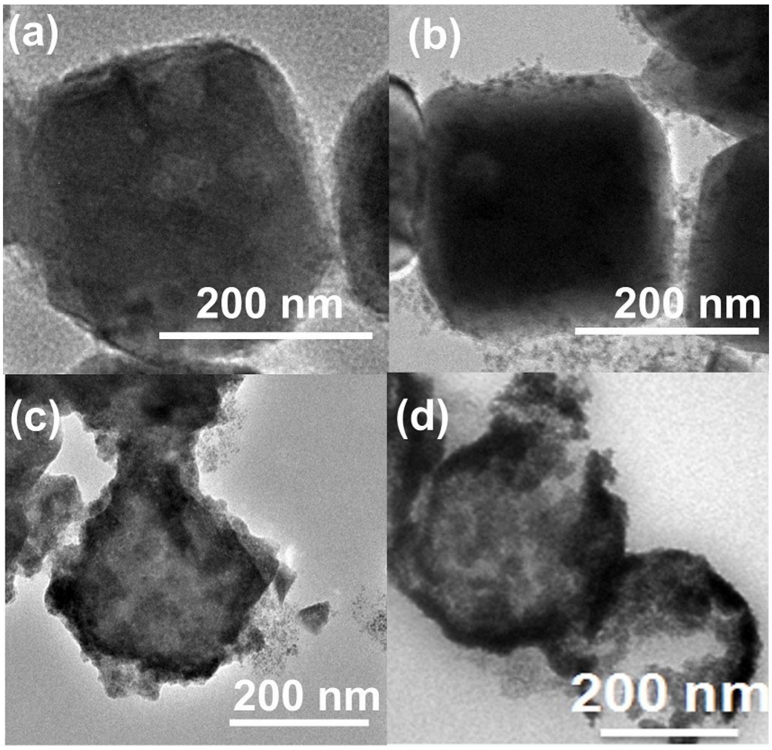

Figure S4: TEM images of Cu_2O@CeO_2 CS-NC(200) with different Ce precursor concentration varying shell thickness. (a) Cu_2O@CeO_2 CS-NC(0.1 mM) showing a very thin shell, (b) Cu_2O@CeO_2 CS-NC(0.4 mM) with a distinct shell but retaining the core, (c) Cu_2O@CeO_2 CS-NC(1.0 mM) shows a complete disrupted shell, (d) broken Pt/CeO_2_NB (200).

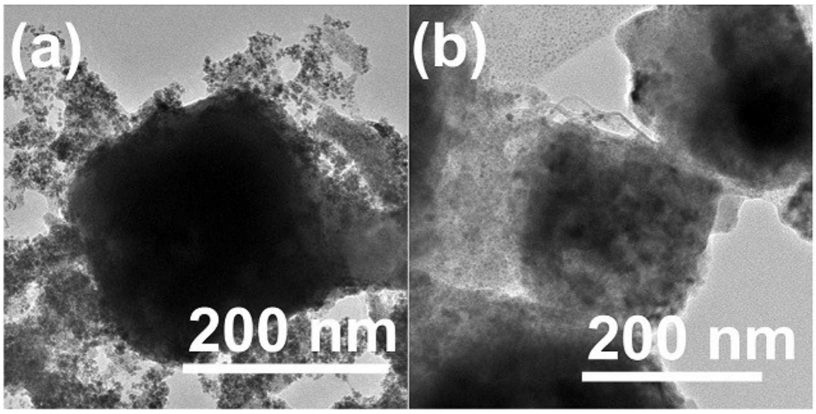

Figure S5: TEM images of Pt/Cu_2O@CeO_2 CS-NC(200) (a) without linker AHA and 40% Pt loading (b) with linker AHA and 20% Pt loading. In both the cases excess Pt is seen in the background.

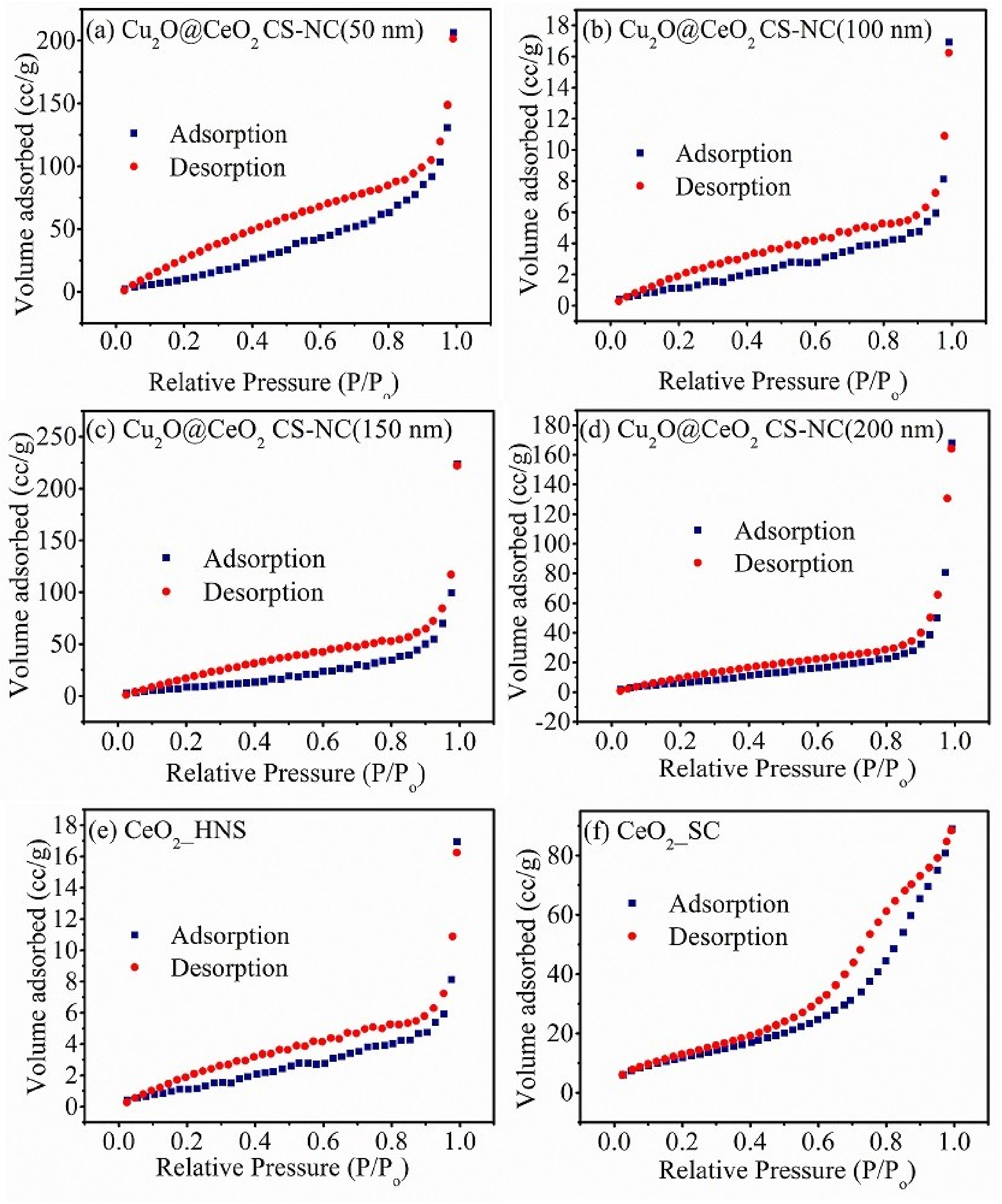

Figure S6. BET absorption desorption curves of different samples.

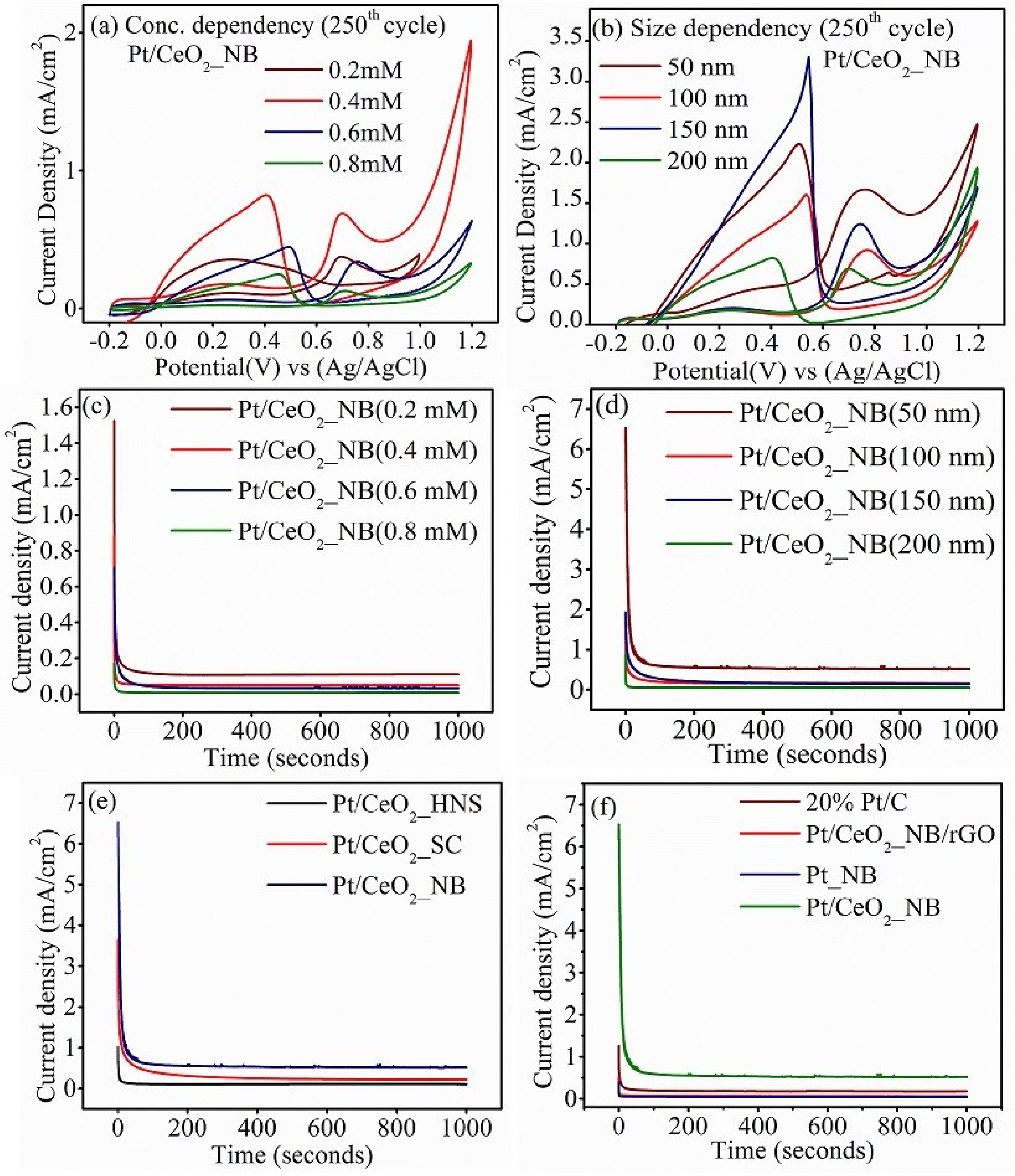

Figure S7. CV and CA curves measured in 0.1 M $HClO_4$ containing 1 M HCOOH for different samples studied. Concentration and size dependent specific activity of samples at 250th cycle over a scan rate of 50 mV/s are represented in (a) and (b), respectively. Concentration, size, and shape dependent chronoamperometric (CA) measurements are shown in (c), (d), (e) and (f), respectively. Figure (f) represents CA comparison of Pt supported on various different supports with commercial Pt/C.

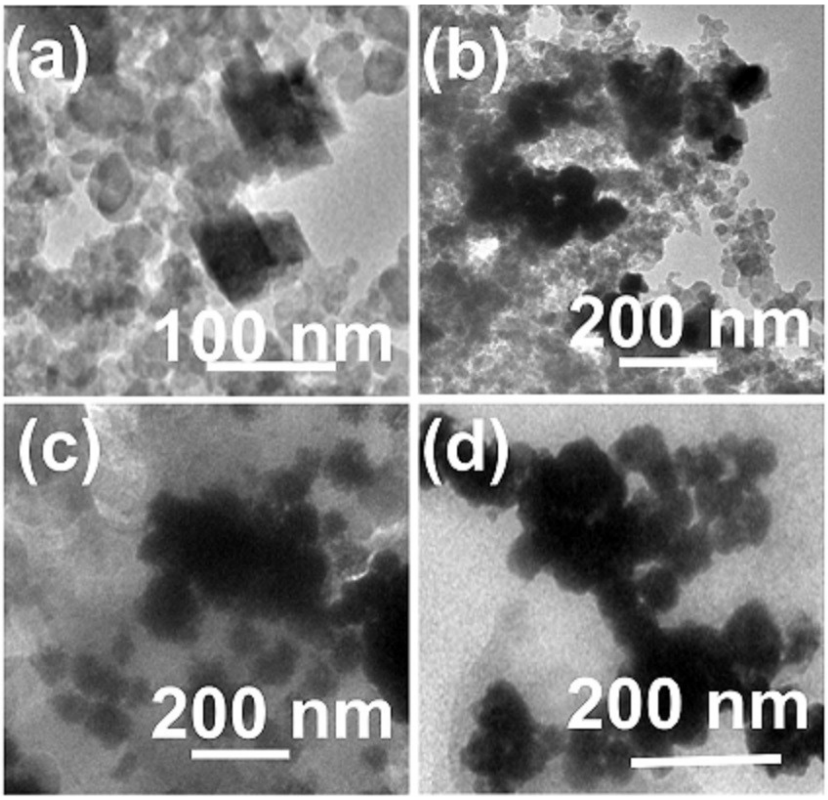

Figure S8. TEM images of electrode slurry (a-b) before and (c-d) after 250 cycles CV measurements showing the presence of Pt/CeO_2_NBs(50)/vulcan.

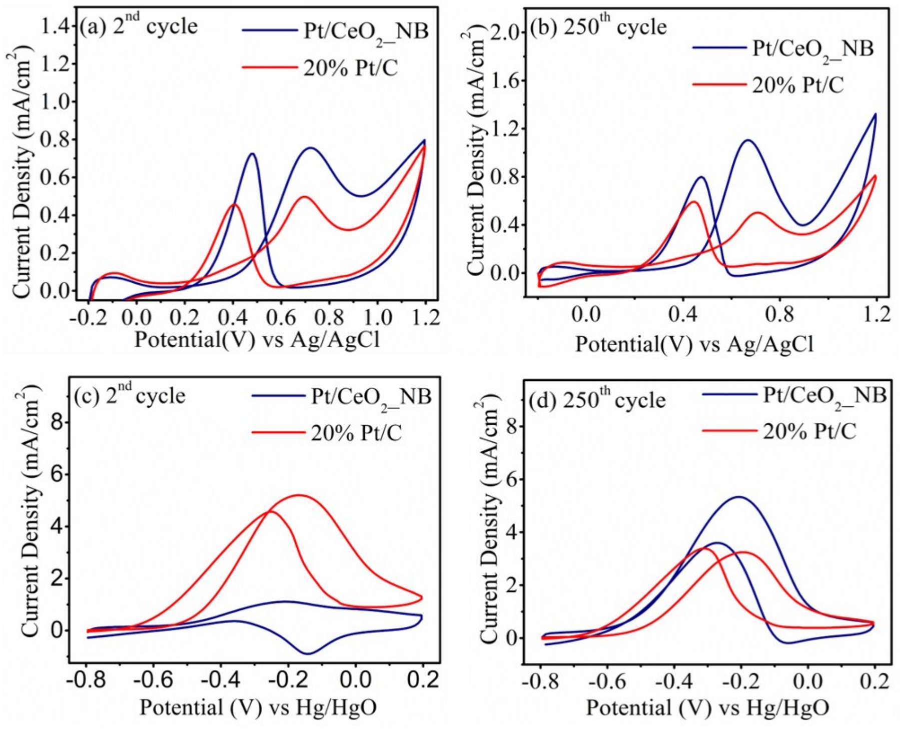

Figure S9. CV curves measured in 0.5 M H_2SO_4/1 M MeOH and 0.5 M KOH/EtOH at a scan rate of 50 mV/s showing specific activity of Pt/CeO_2_NB(50) for MeOH oxidation (a) 2nd cycle (b) 250th cycle and EtOH oxidation (c) 2nd cycle and (d) 250th cycle respectively.

References

1. D.-F. Zhang, H. Zhang, L. Guo, K. Zheng, X.-D. Han and Z. Zhang, *J. Mater. Chem.*, 2009, **19**, 5220-5225.
2. I. C. Chang, P.-C. Chen, M.-C. Tsai, T.-T. Chen, M.-H. Yang, H.-T. Chiu and C.-Y. Lee, *CrystEngComm*, 2013, **15**, 2363-2366.
3. H. Bao, Z. Zhang, Q. Hua and W. Huang, *Langmuir*, 2014, **30**, 6427-6436.
4. Y. Zhiqiang, Z. Kebin, L. Xiangwen, T. Qun, L. Deyi and Y. Sen, *Nanotechnol.*, 2007, **18**, 185606.
5. Z. Yang, D. Han, D. Ma, H. Liang, L. Liu and Y. Yang, *Cryst. Growth Des.*, 2010, **10**, 291-295.
6. W. S. Hummers and R. E. Offeman, *J. Am. Chem. Soc.*, 1958, **80**, 1339-1339.
7. S. Sarkar, R. Borah, A. L. Santhosha, R. Dhanya, C. Narayana, A. J. Bhattacharyya and S. C. Peter, *J. Power Sources*, 2016, **306**, 791-800.
8. T. Binninger, E. Fabbri, R. Kötz and T. J. Schmidt, *J. Electrochem. Soc.*, 2014, **161**, H121-H128.
9. H. Yang, L. Dai, D. Xu, J. Fang and S. Zou, *Electrochim. Acta*, 2010, **55**, 8000-8004.
10. D. Xu, S. Bliznakov, Z. Liu, J. Fang and N. Dimitrov, *Angew. Chem. Int. Edn.*, 2010, **49**, 1282-1285.
11. F. Li, Y. Guo, Y. Liu, H. Qiu, X. Sun, W. Wang, Y. Liu and J. Gao, *Carbon*, 2013, **64**, 11-19.
12. L. Y. Zhang, Z. L. Zhao, W. Yuan and C. M. Li, *Nanoscale*, 2016, **8**, 1905-1909.
13. K. C. Poon, B. Khezri, Y. Li, R. D. Webster, H. Su and H. Sato, *Chem. Comm.*, 2016, **52**, 3556-3559.
14. X. Sun, K. Jiang, N. Zhang, S. Guo and X. Huang, *ACS Nano*, 2015, **9**, 7634-7640.
15. Y. Kang, J. B. Pyo, X. Ye, T. R. Gordon and C. B. Murray, *ACS Nano*, 2012, **6**, 5642-5647.
16. H. J. Qiu, X. Shen, J. Q. Wang, A. Hirata, T. Fujita, Y. Wang and M. W. Chen, *ACS Catal.*, 2015, **5**, 3779-3785.
17. J. Zhang, J. Ma, Y. Wan, J. Jiang and X. S. Zhao, *Mater. Chem. Phys.*, 2012, **132**, 244-247.
18. D. Xu, Z. Liu, H. Yang, Q. Liu, J. Zhang, J. Fang, S. Zou and K. Sun, *Angew. Chem. Int. Edn.*, 2009, **48**, 4217-4221.
19. H. Xu, L.-X. Ding, C.-L. Liang, Y.-X. Tong and G.-R. Li, *NPG Asia Mater*, 2013, **5**, e69.
20. S. W. Kang, Y. W. Lee, Y. Park, B.-S. Choi, J. W. Hong, K.-H. Park and S. W. Han, *ACS Nano*, 2013, **7**, 7945-7955.
21. A.-X. Yin, X.-Q. Min, Y.-W. Zhang and C.-H. Yan, *J. Am. Chem. Soc.,* 2011, **133**, 3816-3819.
22. B. T. Sneed, A. P. Young, D. Jalalpoor, M. C. Golden, S. Mao, Y. Jiang, Y. Wang and C.-K. Tsung, *ACS Nano*, 2014, **8**, 7239-7250.
23. A. Kowal, M. Li, M. Shao, K. Sasaki, M. B. Vukmirovic, J. Zhang, N. S. Marinkovic, P. Liu, A. I. Frenkel and R. R. Adzic, *Nat. Mater.*, 2009, **8**, 325-330.